

Application of Computational Model Updating to Aeroengine Components

C. Schedlinski
ICS, Langen, Germany
e-mail: sched@t-online.de

M. Link
Lightweight Structures and
Structural Mechanics Laboratory,
University of Kassel, Germany
e-mail : link@hrz.uni-kassel.de

A. Schönrock
BMW Rolls-Royce, Dahlewitz,
Germany
e-mail :
Armin.Schoenrock@brr.de

Abstract

In this paper the application of a computational model updating procedure to aeroengine components is presented. A special MATLAB based software developed at the University of Kassel, Lightweight Structures and Structural Mechanics Laboratory, was applied. This software utilizes as much as possible of the analysis capacities of the FE-code MSC/NASTRAN, in particular the sensitivity module which allows to handle large order FE-models. Main goal was to improve the confidence in the predictions coming from the complex 'Whole Engine Model (WEM)'. The concept applied is based on updating the FE-models of engine components using experimental modal data of the components which allows to restrict the number of uncertain parameters of the WEM. The different steps performed during the model development are presented by example of one representative component. Then the results for the other investigated components are summarized and the correlation of the WEM to experimental modal data is presented in order to verify the effectiveness of the utilized concept.

1. Introduction

Aeroengines are complex technical systems, which have to meet the highest requirements with regard to reliability, manufacturing costs, fuel consumption, weight, noise, emissions and other important criteria.

The optimization of the aircraft installed turbomachinery's structural behavior has a considerable influence on the performance of the whole aircraft. At BMW Rolls-Royce AeroEngines the simulation of this complex system within its flight and landing envelopes is performed using a so called 'Whole Engine Model (WEM)' (figure 1) under application of MSC/NASTRAN.

These simulations are a significant contribution to the determination of internal load and deformation distributions under static and dynamic loading conditions. Static loads are generated by thrust, maneuver and landing conditions, etc. Dynamic loads cover nonlinear transient conditions like bird impact, blade failures and windmilling. Engine dynamics, carcass vibrations and critical speeds are part of the rotordynamic analyses required in an engine certification process.

It is obvious that the accuracy of the model predictions is critical for the ambitious task the WEM has to fulfill in this optimization process. Additionally in order to reduce the amount of destructive testing modern aeroengine manufacturers intend to supersede this cost and lead time producing approach by simulations with validated numerical models.

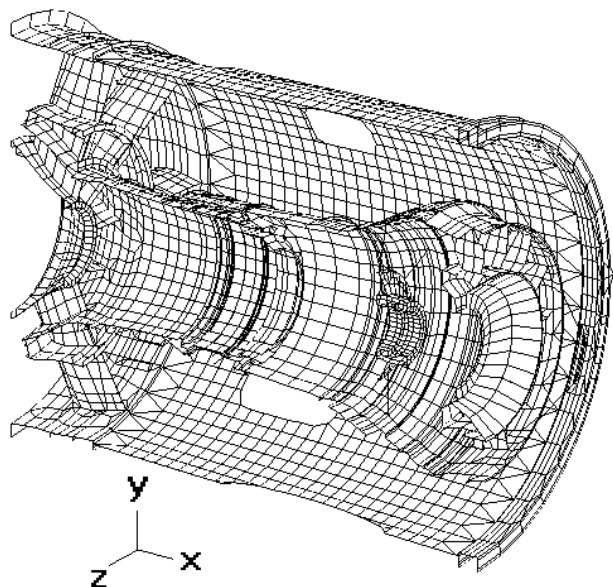


Figure 1: Section cut through WEM w/o rotor

Experimental modal analysis (EMA) results, i.e. natural frequencies and mode shapes identified from vibration test data, are often used to assess the quality of FE-analysis predictions. If the deviations between identified and predicted data are large, a modification of the FE-model structure may become necessary, i.e. the structural idealizations must be reviewed. If the model structure is suitable parametric studies based on engineering experience may be performed to reduce the test/analysis deviations. However, if the number of parameters becomes too large it is often impossible to assess easily the effects of parameter changes on the FE-analysis results. Then computational model updating procedures must be used instead. These procedures are capable of tuning several parameters simultaneously such that the deviations of identified and predicted natural frequencies and mode shapes are minimized.

In this paper the application of a computational model updating procedure to aeroengine components is presented. A special MATLAB based software developed at the University of Kassel, Lightweight Structures and Structural Mechanics Laboratory (UKL), was applied. This software utilizes as much as possible of the analysis capacities of the FE-code MSC/NASTRAN, in particular the sensitivity module which allows to handle large order FE-models.

Main goal was to validate the complex WEM. The concept is based on updating the FE-models of engine components using experimental modal data of the components. This allows to restrict the number of uncertain parameters of the WEM.

The different steps performed during the model development (test design, conduction and evaluation, selection of the most effective update parameters and the automated updating using the classical inverse modal sensitivity approach) are presented by example of one representative component. In addition the results for the other investigated components are summarized and the correlation of the WEM to experimental modal data is presented in order to verify the effectiveness of the applied concept.

2. Updating Theory

The basis for the used computational model updating software is the following parameterization of the model matrices (see references [1], [2]):

$$\mathbf{K} = \mathbf{K}_A + \sum \alpha_i \mathbf{K}_i \quad , \quad i = 1 \dots n_\alpha \quad (1a)$$

$$\mathbf{M} = \mathbf{M}_A + \sum \beta_j \mathbf{M}_j \quad , \quad j = 1 \dots n_\beta \quad (1b)$$

with:

$\mathbf{K}_A, \mathbf{M}_A$ initial analytical stiffness/mass matrices
 $\mathbf{p} = [\alpha_i \beta_j]$ vector of unknown design parameters
 $\mathbf{K}_i, \mathbf{M}_j$ given substructure matrices defining location and error of model uncertainties

This parameterization allows for local updating of uncertain model areas. Using equations (1) and appropriate residuals (containing different test/analysis differences) the following objective function J can be derived:

$$J(\mathbf{p}) = \Delta \mathbf{z}^T \mathbf{W} \Delta \mathbf{z} + \mathbf{p}^T \mathbf{W}_p \mathbf{p} \rightarrow \min \quad (2)$$

with: $\Delta \mathbf{z}$ residual vector
 \mathbf{W}, \mathbf{W}_p weighting matrices

The minimization of equation (2) yields the desired design parameters \mathbf{p} . The second term in equation (2) is used to constrain the parameter variation. The weighting matrix \mathbf{W}_p has to be selected with care since for $\mathbf{W}_p \gg \mathbf{0}$ no design parameter changes will occur.

The residuals $\Delta \mathbf{z} = \mathbf{z}_T - \mathbf{z}(\mathbf{p})$ (\mathbf{z}_T : test data vector, $\mathbf{z}(\mathbf{p})$: corresponding analytical data vector) usually depend in a nonlinear way on the design parameters. Thus the minimization problem is also nonlinear and must be solved iteratively. One way is to use the classical sensitivity approach (see reference [3]) where the analytical data vector is linearized at point 0 by a Taylor series expansion truncated after the first term. Proceeding this way leads to:

$$\Delta \mathbf{z} = \Delta \mathbf{z}_0 - \mathbf{G}_0 \Delta \mathbf{p} \quad (3)$$

with:

$\Delta \mathbf{p} = \mathbf{p} - \mathbf{p}_0$ design parameter change
 $\Delta \mathbf{z}_0 = \mathbf{z}_T - \mathbf{z}(\mathbf{p}_0)$ test/analysis difference at linearization point 0
 $\mathbf{G}_0 = \partial \mathbf{z} / \partial \mathbf{p}|_{\mathbf{p}=\mathbf{p}_0}$ sensitivity matrix at linearization point 0
 \mathbf{p}_0 design parameter vector at linearization point 0

If the design parameters are not bounded the minimization problem (2) leads to the linear problem (4) which has to be solved in each iteration step for the actual linearization point.

$$(\mathbf{G}_0^T \mathbf{W} \mathbf{G}_0 + \mathbf{W}_p) \Delta \mathbf{p} = \mathbf{G}_0^T \mathbf{W} \Delta \mathbf{z}_0 \quad (4)$$

For $\mathbf{W}_p = \mathbf{0}$ equation (4) represents a standard weighted least squares problem. It shall be mentioned that any other mathematical minimization technique may as well be used to solve equation (2).

The residuals used in the computational model updating software are natural frequency and mode shape residuals. I.e. the analytical modal analysis results are subtracted from the corresponding EMA results. The residual vector in this case takes the form:

$$\Delta \mathbf{z}_0 = \begin{bmatrix} \omega_T - \omega \\ \mathbf{x}_T - \mathbf{x} \end{bmatrix}_0 \quad (5)$$

with:

ω_T, ω_0 test/analysis vectors of natural frequencies
 \mathbf{x}_T, \mathbf{x} test/analysis mode shape vectors

The sensitivity matrix for the residual vector introduced in equation (5) is given in equation (6).

$$\mathbf{G}_0 = \begin{bmatrix} \partial \omega / \partial \mathbf{p} \\ \partial \mathbf{x} / \partial \mathbf{p} \end{bmatrix}_0 \quad (6)$$

For the calculation of the derivatives please refer to references [1], [2].

3. Model Development Procedure

Five engine components which were considered important for the overall structural mechanical behavior were selected for investigation: Intermediate Casing (IMC), Bypass Duct (BPD), Rear Mount Ring (RMR), High Pressure Compressor Split Casings (HPCS) and High Pressure Compressor Rear Outer Casing (HPCROC), figure 2.

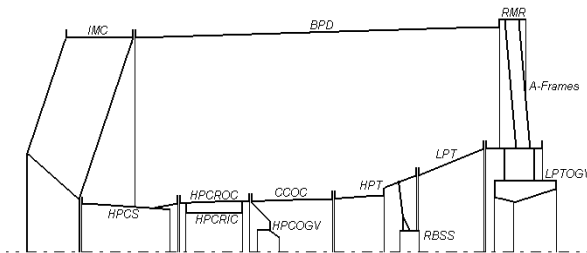


Figure 2: Survey of components

The components High Pressure Turbine Casing (HPT) and Rear Bearing Support Structure (RBSS) have already been validated in an earlier step (see reference [4]) and are not the subject of this paper.

The model development procedure is presented in the following by example of the IMC.

3.1 Test design

In order to acquire adequate information about the IMC during the test, test design was performed using the IMC FE-model (figure 3). The test design covered the following aspects:

- selection of target modes
- selection of measurement degrees of freedom (MDOF) w. r. t.:
 - coincidence of MDOF and FE-DOF
 - sufficient spatial resolution of the target modes
- selection of exciter locations
- adequate frequency resolution

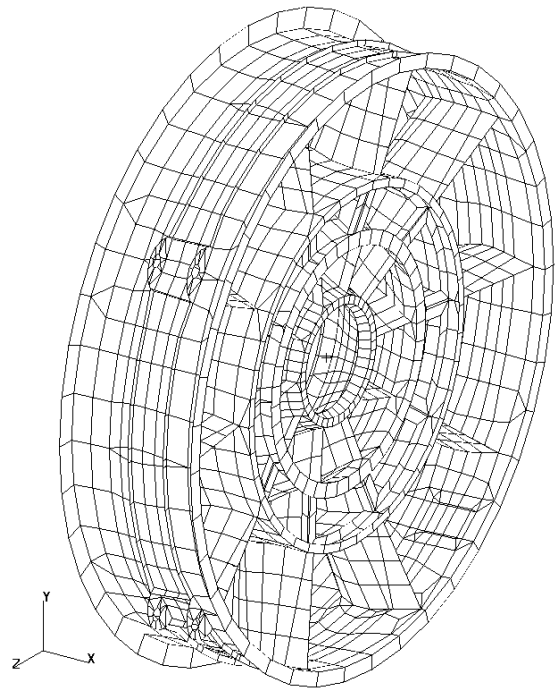


Figure 3: IMC FE-model

Selection of target modes

In order to gather sufficient information w. r. t. the global stiffness of the IMC all global elastic modes in the frequency range from 0 to 500 Hz were chosen as target modes (local modes of the spokes were not considered). I.e. these modes were to be excited and observed in the test. Above that, it was decided to provide sufficient spatial resolution of all elastic modes from 0 to 500 Hz in order to avoid spatial aliasing problems in any case.

Selection of MDOF

Selection of MDOF was performed in three steps:

1. principal assessment of required measurement information
2. selection of MDOF based on coincidence with FE-nodes and accessibility
3. check of validity of selected MDOF

The principal assessment of necessary measurement information was made utilizing ICS/UKL in-house pickup-selection software which is based on a maximum linear independence criterion of the mode shapes (please see reference [5]). All elastic modes up to 500 Hz were considered.

It was found that the mode shapes can primarily be described by radial MDOF on the outer ring and tangential MDOF on the spokes of the IMC. In order to allow for visualization as well the following MDOF were chosen:

- outer flange - front: 10 radial responses
- outer flange - rear: 10 radial responses
- inner flange - front: 10 radial responses
- splitter box - rear: 10 radial responses
- spokes: 20 tangential responses

The validity of the selected MDOF was checked by calculating the Auto-MAC of the target modes at the selected MDOF. It was found that the measurement information was sufficient and provided nearly linear independent mode shapes. Only two mode pairs in the frequency range above 350 Hz showed relatively high correlation. However, the frequencies of the corresponding shapes were separated by about 140 Hz. Thus a pairing problem was not to be expected. The test model is shown in figure 4.

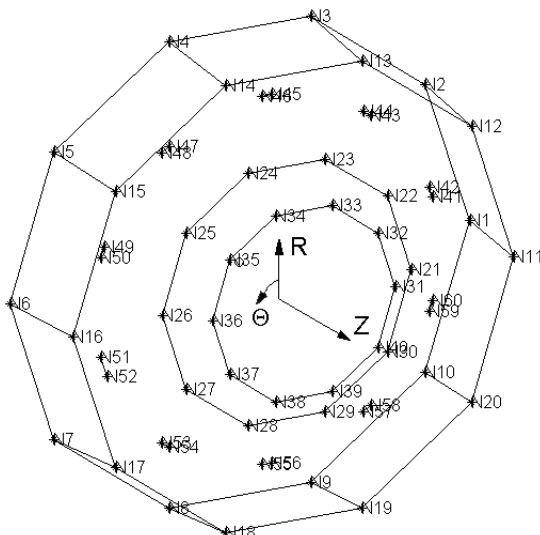


Figure 4: IMC test model

Selection of exciter locations

In order to determine the optimal exciter locations response calculations were made using the selected MDOF. Possible exciter locations were pre-selected w.r.t. their ability to excite the target modes using ICS/UKL in-house exciter-selection software (please see reference [5]). For each possible exciter location univariate mode indicator functions (MIF) were calculated according to [6]. Based on these MIFs three exciter locations were chosen such that every target mode may be excited by at least one of the exciters. Proceeding this way led to two radial exciter locations on the rear outer flange and one tangential exciter locations on the spoke at 162°. These exciter locations represent the minimum configuration necessary to sufficiently excite the target modes.

Frequency resolution

The first mode is found at approximately 128 Hertz in the FE-analysis. If modal damping of 0.5 % is assumed for this mode, it was found from response calculations that a frequency spacing less than 0.5 Hertz was appropriate in order to provide sufficient resolution.

3.2 Vibration Test

For the vibration test the IMC was suspended by bungee cords to simulate free/free boundary conditions, figure 5. The MDOF found above were used for the test and three reference accelerometers were placed at the chosen exciter locations. The IMC was then excited by an impact hammer.



Figure 5: IMC test setup

3.3 EMA Results

The results of the EMA are summarized in table 1.

Table 1: IMC EMA results

no.	freq. [Hz]	modal damping [%]	no.	freq. [Hz]	modal damping [%]
1	127.38	1.01	16	385.28	0.28
2	132.64	0.22	17	393.85	0.37
3	195.78	0.15	18	413.33	0.05
4	213.36	0.98	19	444.81	0.13
5	225.31	0.49	20	477.06	0.26
6	242.04	0.13	21	535.71	0.44
7	249.12	0.47	22	546.50	0.16
8	310.14	0.11	23	554.06	0.20
9	311.80	0.08	24	558.60	0.16
10	326.33	0.16	25	566.36	0.17
11	341.36	0.20	26	569.37	0.09
12	348.10	0.15	27	575.23	0.14
13	351.44	0.10	28	586.38	0.55
14	355.08	0.12			
15	379.35	0.22			

3.4 Computational Model Updating

The initial correlation of the IMC to EMA data is listed in table 2 and the corresponding MAC matrix is visualized in figure 6.

Table 2: IMC initial correlation

FEA no.	EMA no.	freq. [Hz]		deviation [%]	MAC [%] (> 60 %)
		FEA	EMA		
1	1	128.15	127.38	0.61	94.75
2	2	136.71	132.64	3.07	95.05
3	3	152.64	195.78	-22.03	89.11
4	4	236.47	213.36	10.83	90.79
6	5	241.96	225.31	7.39	63.92
5	6	236.83	242.04	-2.15	79.06
7	7	243.57	249.12	-2.23	85.09
8	8	304.01	310.14	-1.97	68.21
9	9	304.95	311.80	-2.20	66.62
12	12	332.82	348.10	-4.39	62.47
13	15	336.81	379.35	-11.21	63.13
23	18	421.79	413.33	2.05	89.59
25	19	469.53	444.81	5.56	81.70
26	20	484.31	477.06	1.52	65.00

Only 14 of 28 identified mode shapes could be paired. In addition analytical mode three exhibits a very large frequency deviation. Mode three is a global torsional mode where the outer ring of the IMC rotates against the inner IMC part. From this it may be concluded that the stiffness of the IMC spokes is higher than modeled.

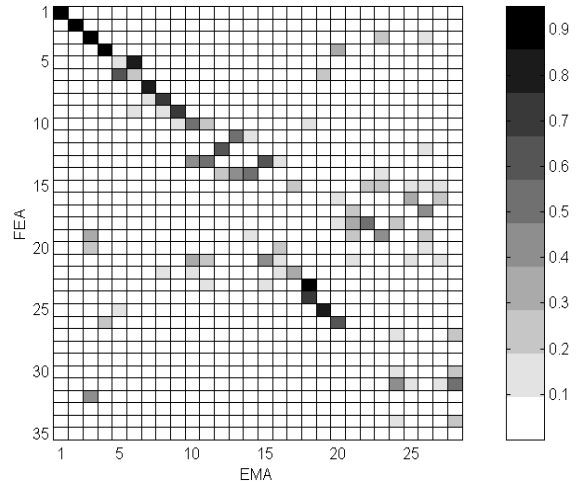


Figure 6: IMC initial MAC matrix test vs. analysis

In order to determine the most sensitive design parameters a sensitivity study was conducted. To do so the sensitivity matrix according to eq. (6) was calculated for multiple design parameters (Youngs Moduli of shell elements, shell thicknesses, etc.). It showed that the outer ring region and the spoke region between outer ring and the so called splitter box (see figure 7) were more sensitive than other model regions. Therefore updating was focused on design parameter changes of these regions. It shall be emphasized that a sensitivity study does not allow to assess the physical relevance of a design parameter. It merely reflects a design parameter's potential to change the modal behavior of the model.

It was decided to use shell thickness parameters for updating only because the physical interpretation of thickness changes is obvious and the validity of such changes is easier to asses. Various updating runs were performed using different design parameter sets. In all cases the thickness changes of the spokes were quite extensive indicating that some systematic modeling problem is present here. The smallest spoke thickness change could be produced by updating the whole spoke region between outer ring and splitter box with only one parameter. Updating runs where the inner spoke region was updated independently from the areas where the spokes are connected to outer ring and splitter box (in order to account for fillets in the connection areas) did not yield satisfactory results.

The results of the updating run providing the smallest parameter variations are presented in figure 8. Here the three major regions on the outer shell (P1) were updated as well as the spoke thicknesses between outer ring and splitter box (P2); see figure 7 for a survey of the parameter locations.

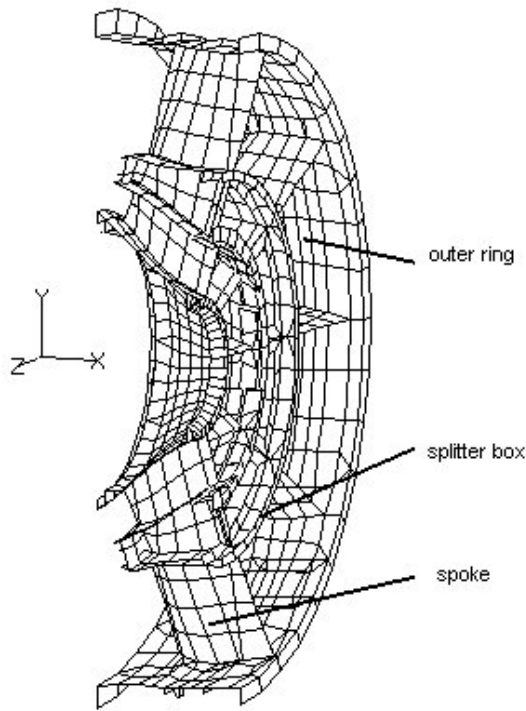


Figure 7: IMC design parameter locations

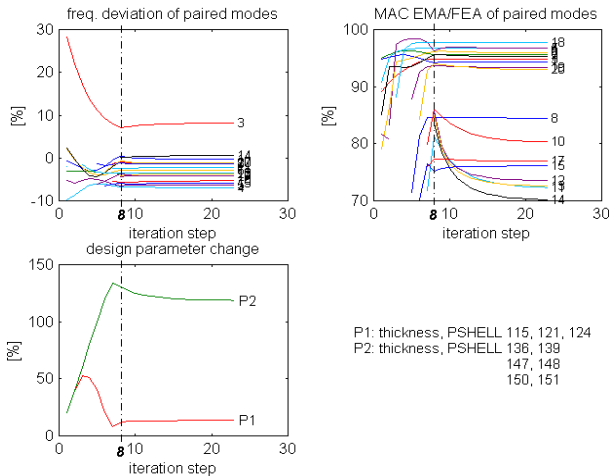


Figure 8: IMC computational updating results

The frequency deviations and MAC values improve until iteration step 8 and become worse thereafter. Since every iteration step represents a physically interpretable result it was decided to use the iteration step 8 results as the final results. The correlation after iteration step 8 of the IMC model to BRR test data is listed in table 3 and the corresponding MAC matrix is visualized in figure 9.

After iteration step 8 all EMA modes except for mode 16 can be paired to analysis results with high MAC values. Moreover the frequency deviation is effectively reduced to maximal 7.27 % instead of -22.03 % before update. Since all paired modes are global modes of the IMC the global behavior has obviously been improved significantly. However,

after update no local out of plane modes of the spokes are paired anymore. This indicates that the updated spoke thicknesses are only substitute design parameters in order to tune the modal behavior of the model. If static/dynamic displacement or modal analysis calculations are to be conducted this is acceptable. If, on the other hand, stress analysis is to be performed the results in the updated spoke areas may lose their physical relevance.

Table 3: IMC correlation after iteration step 8

FEA no.	EMA no.	freq. [Hz]		deviation [%]	MAC [%] (> 60 %)
		FEA	EMA		
1	1	127.27	127.38	-0.08	94.25
2	2	137.61	132.64	3.75	95.60
3	3	182.43	195.78	-6.82	94.88
4	4	228.88	213.36	7.27	96.76
5	5	240.64	225.31	6.80	96.84
6	6	249.35	242.04	3.02	96.21
7	7	252.05	249.12	1.18	95.56
8	8	314.10	310.14	1.28	84.68
9	9	325.90	311.80	4.52	68.86
10	10	346.02	326.33	6.03	84.76
11	11	349.65	341.36	2.43	78.94
13	12	362.89	348.10	4.25	79.38
14	13	366.01	351.44	4.15	79.09
12	14	354.28	355.08	-0.23	78.51
17	15	403.76	379.35	6.44	75.71
16	17	398.18	393.85	1.10	77.30
18	18	428.78	413.33	3.74	97.70
19	19	463.28	444.81	4.15	93.61
20	20	481.77	477.06	0.99	93.88

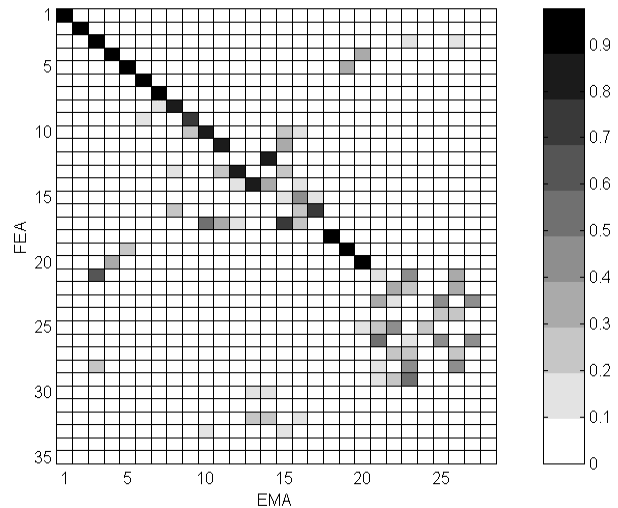


Figure 9: IMC MAC matrix test vs. analysis after iteration step 8

3.5 Updating of other components

The other components were treated in the same manner as the IMC. Only the HPCROC was not

subjected to computational model updating since it already correlated very well with the EMA data.

The correlation before and after computational model updating is presented in tables 4, 5, 6 and 7. BPD and RMR were treated as one unit, thus appearing in one table only. The results of the corresponding computational model updating runs are presented in figures 10 and 11.

Table 4: HPCS initial correlation

FEA no.	EMA no.	freq. [Hz]		deviation [%]	MAC [%] (> 60 %)
		FEA	EMA		
4	2	143.76	130.69	10.00	78.71
1	4	131.96	168.28	-21.58	78.89
5	5	358.26	343.77	4.22	81.41
6	6	365.68	354.29	3.22	73.11
8	7	418.07	465.22	-10.14	85.70
7	8	413.02	484.04	-14.67	81.80
9	9	609.63	612.48	-0.46	84.27
10	10	633.39	641.76	-1.30	96.23
11	11	762.02	835.60	-8.81	69.52
14	13	937.40	988.49	-5.17	68.41
19	18	1205.55	1257.64	-4.14	73.51

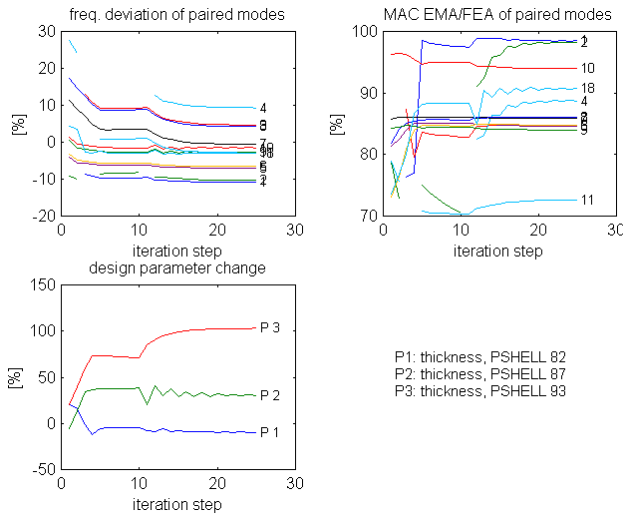


Figure 10: HPCS computational updating results

After update the first 10 EMA modes of the HPCS can be paired to analysis results with MAC values greater than 80 %. Furthermore the maximal frequency deviation is reduced from -21.58 % to 12.10 %. However, the first four analytical modes still lie within a frequency range of 10 Hz width, the corresponding EMA modes on the other hand within a frequency range of 40 Hz width. This indicates some systematic problem due to local effects not entirely modeled and represented by the chosen design parameters.

Table 5: HPCS correlation after update

FEA no.	EMA no.	freq. [Hz]		deviation [%]	MAC [%] (> 60 %)
		FEA	EMA		
1	1	143.24	127.78	12.10	98.48
2	2	145.55	130.69	11.38	98.23
4	3	156.97	164.28	-4.45	84.74
3	4	153.94	168.28	-8.52	88.68
5	5	369.56	343.77	7.50	84.62
6	6	378.89	354.29	6.94	84.78
8	7	467.72	465.22	0.54	85.88
7	8	464.23	484.04	-4.09	86.07
9	9	629.54	612.48	2.79	84.00
10	10	651.59	641.76	1.53	93.93
11	11	860.17	835.60	2.94	72.58
14	13	968.44	988.49	-2.03	64.09
22	18	1296.28	1257.64	3.07	90.79

Table 6: BPD/RMR initial correlation

FEA no.	EMA no.	freq. [Hz]		deviation [%]	MAC [%] (> 60 %)
		FEA	EMA		
4	1	16.54	15.78	4.86	78.57
5	2	16.92	15.91	6.35	72.96
7	3	44.05	40.33	9.23	97.62
6	4	42.58	42.78	-0.45	97.32
8	5	47.01	45.65	2.98	81.52
9	6	50.33	49.83	1.01	84.88
11	7	76.15	70.60	7.86	92.24
10	8	74.45	76.30	-2.43	93.90
12	9	96.52	94.67	1.96	88.94
13	10	107.27	108.88	-1.48	87.77
14	11	116.75	115.41	1.16	81.36
15	12	121.04	118.44	2.20	88.29
16	13	122.19	121.46	0.60	71.58
23	20	168.88	166.33	1.53	71.07

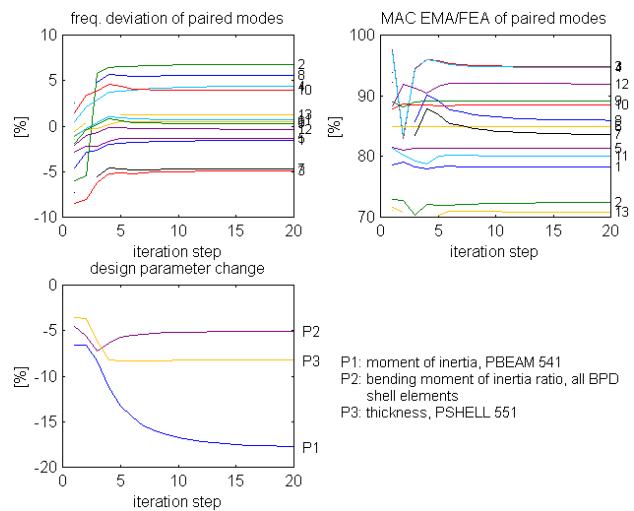


Figure 11: BPD computational updating results

Table 7: BPD correlation after update

FEA no.	EMA no.	freq. [Hz]		deviation [%]	MAC [%] (> 60 %)
		FEA	EMA		
4	1	16.03	15.78	1.59	78.23
3	2	14.90	15.91	-6.36	72.40
7	3	42.41	40.33	5.17	94.77
6	4	40.98	42.78	-4.19	94.63
8	5	46.26	45.65	1.35	81.34
9	6	49.58	49.83	-0.50	84.85
11	7	74.08	70.60	4.92	83.63
10	8	72.29	76.30	-5.26	85.96
12	9	94.43	94.67	-0.25	89.21
13	10	104.78	108.88	-3.77	88.48
14	11	114.61	115.41	-0.69	80.00
15	12	118.83	118.44	0.33	91.97
16	13	119.98	121.46	-1.22	70.83
23	20	165.08	166.33	-0.75	67.57

A comparison of table 7 with table 6 shows that no significant improvement of the MAC values occurred. However, the maximal frequency deviation could be reduced from 9.23 % before update to -6.36 % after update.

3.6 Correlation of WEM to EMA data

A vibration test using the WEM w/o rotor and dressings was performed in order to obtain EMA data to be used for correlation. The EMA provided mode shapes from two radial, one tangential and one axial reference. From these mode shapes a subset was extracted holding mainly global modes that were considered to be of acceptable accuracy.

The updated components on the other hand were inserted into the WEM and the results of the analytical modal analysis were compared to the EMA data; table 8.

Table 8: WEM correlation with selected modes

FEA no.	EMA no.	freq. [Hz]		deviation [%]	MAC [%] (> 50 %)
		FEA	EMA		
3	1	94.44	93.21	1.31	93.36
2	2	94.31	99.56	-5.27	55.01
4	3	102.26	102.92	-0.64	88.58
5	4	104.53	106.24	-1.61	80.27
8	5	112.84	113.02	-0.16	92.49
9	6	118.90	115.65	2.81	84.53
13	8	132.35	136.58	-3.09	87.18
10	10	125.33	141.10	-11.18	81.39
21	11	171.15	174.28	-1.80	61.62
26	14	185.48	211.17	-12.16	60.26
40	17	230.74	241.40	-4.42	67.45

The first six and some higher EMA modes could be paired to analysis results. The first analytical mode, however, was obviously not identified. A visual

check of this mode showed that it is a local BPD mode and was therefore probably not excited in the test. The overall frequency deviation is already acceptable. Only for FE-modes 10 and 26 the deviations are higher. Above 200 Hz only two modes could be paired.

4. Conclusions

The computational updating of components provided component models that better reproduce the modal behavior of the real structures especially in the lower frequency range. Subsequently these updated models were inserted into the WEM.

Altogether the procedure applied has proven to be quite effective. The investigation of the components in advance reduced the number of uncertain parameters to be considered for the assembly. By this way an acceptable correlation between global test and analysis modes could be achieved in the frequency range up to 200 Hz. Thus the engineering accuracy of the updated model can be considered validated in this frequency range. Finally, it shall be emphasized that only design parameters were used that were physically meaningful, which increases the confidence in the updated model.

References

1. M. Link et al., *Baudynamik und Systemidentifikation*, in: Der Ingenieurbau, Grundwissen, [5] Baustatik, Baudynamik, Hrsg. G. Mehlhorn, Ernst & Sohn, Berlin, 1995
2. H. G. Natke, *Einführung in die Theorie und Praxis der Zeitreihen- und Modalanalyse*, 3., überarb. Aufl., Vieweg Verlag, Braunschweig; Wiesbaden, 1992
3. J. D. Collins et al., *Statistical Identification Of Structures*, AIAA J., Vol. 12, No. 2, pp. 185-190; 1974
4. M. Link/G. Hanke, *Model Quality Assessment and Model Updating*, Proc. of the NATO Advanced Study Institute, Sesimbra, Portugal, May 1998
5. C. Schedlinski/M. Link, *An Approach to Optimal Pick-Up and Exciter Placement*, Proc. of the 14th IMAC, Dearborn, Michigan, USA; 1996
6. E. Breitbach, *Neuere Entwicklungen auf dem Gebiet des Standschwingungsversuchs an Luft- und Raumfahrtstrukturen*, VDI-Bericht Nr. 221, 1997